Heliyon 10 (2024) e38852

Contents lists available at ScienceDirect

Heliyon

journal homepage: www.cell.com/heliyon

Research article

Effect of binary porogen mixtures on polymer monoliths prepared by gamma-radiation initiated polymerization

Barbara Beiler [a,*], Ágnes Sáfrány [b], Lilia Bató [a], Zsombor Szomor [a], Miklós Veres [c]

[a] *Institute of Technical Physics and Materials Science, HUN-REN Centre for Energy Research, PO Box 49, H-1525, Budapest, Hungary*
[b] *Radiation Chemistry Department, HUN-REN Centre for Energy Research, PO Box 49, H-1525, Budapest, Hungary*
[c] *Institute for Solid State Physics and Optics, HUN-REN Wigner Research Centre for Physics, PO Box 49, H-1525, Budapest, Hungary*

ARTICLE INFO

Keywords:
Porous polymer monolith
Gamma-radiation initiated polymerization
Binary porogen
Polymerization rate
Growth mechanism

ABSTRACT

Gamma-radiation initiated polymerization is an easy-to-use and simple technique for the preparation of porous polymer monoliths widely used as active materials in separation columns. Herein, binary porogen mixtures of ethyl acetate/acetone/acetonitrile with methanol were used to synthesize diethylene glycol dimethacrylate monoliths with this technique. Systematic studies have been performed to determine the effect of the composition of the solvent mixture on the morphology and the reaction kinetics, including the growth mechanism and the growth rate. The irradiation dose-dependent conversion profiles showed that with binary solvents the polymerization is much faster than with the same compounds used as single solvents. Depending on the type and the composition of the solvent one-, two- and three-dimensional, and fractal growth mechanisms were identified.

1. Introduction

Porous polymer monoliths (bulk polymers with pores formed during the polymerization) have gained significant attention in recent years due to their unique properties and versatile applications in various fields. These three-dimensional structures with interconnected pores exhibit a high surface area, mechanical stability, and tunable porosity, making them suitable for applications such as chromatography, catalysis, adsorption, and drug delivery [1–6]. Tailoring the properties of monoliths, including the pore size and distribution, connectivity and surface characteristics is a critical step for their applications.

Gamma radiation-initiated polymerization is widely used to prepare porous polymer monoliths [7–13]. Its main advantages over the conventional thermal or UV initiated [14–16] approaches include the absence of initiators and other additives (since the radiation produces radicals directly on the monomer), temperature-independence, and the broad size and shape options for molding [17,18]. This method allows the synthesis of the media for chromatographic separations directly in the column container. In the simplest form of gamma radiation-initiated polymerization the monomer mixture is composed of only the solvent (porogen) and the monomer. With this technique structures ranging from non-porous to macroporous can be obtained changing only the type of the solvent [19–23].

Obviously, dose is a crucial parameter determining the degree of conversion and cross-linking during gamma radiation-initiated polymerization. It has to be large enough to ensure high levels of the degree of conversion (usually >90 %). The process is also affected by the dose rate determining the rate of free radical formation, and so the rate of polymerization and cross-linking [8].

---

[*] Corresponding author.

E-mail addresses: beiler.barbara@ek.hun-ren.hu (B. Beiler), asafrany@mac.com (Á. Sáfrány), bato.lilia@ek.hun-ren.hu (L. Bató), szomor.zsombor@ek.hun-ren.hu (Z. Szomor), veres.miklos@wigner.hun-ren.hu (M. Veres).

https://doi.org/10.1016/j.heliyon.2024.e38852
Received 21 March 2024; Received in revised form 1 September 2024; Accepted 1 October 2024

Among other factors such as polymerization time [24], monomer concentration [6], temperature [25,26] etc. the selection of the solvent (porogen) plays a crucial role in the morphology, pore size and volume, and mechanical stability of the resultant monolith [6, 24]. The main criteria to the porogen are [24]: it must be inert, not polymerizing or reacting with the monomer, or other components of the polymerization mixture; it must be compatible with the initiation method; in case of using more than one porogen, they must be miscible with each other and able to form a homogeneous solution when mixed with the monomers and the crosslinkers.

The main mechanism behind the porous monolith structure formation is the precipitation polymerization [8–10]. The gamma radiation activates the monomers and their crosslinking results in formation of polymer nuclei. After reaching a certain size these nuclei precipitate from the monomer mixture and the polymerization is concentrated on their surface [27,28]. Subsequently, the growing nuclei connect with each other and merge into a porous structure. During this process the selection of the solvent influences mainly two parameters: the material transport in the monomer mixture and the precipitation [8–10]. The first affects the growth rate of the polymer, while the second – the porous structure. If the porogen facilitates early precipitation of the nuclei, large structural unit will merge leaving voids between them and thus forming a porous polymer; on the other hand, the absence of precipitation will result in a bulk or nanoporous structure. As our previous studies showed, the efficiency of the porogen depends on the dose rate [8]. The latter affects the rate of polymerization and cross-linking, and therefore, the phase separation. For the same monomer mixture composition higher dose rates will result in earlier phase separation and so in larger nuclei and bigger pores between them.

It was shown that the process occurring in a given monomer mixture is governed by the relation between the solubilities of the monomer and the solvent [8,9,29]. In case of methacrylate monomers the use of alcohols as porogenic solvent resulted in monoliths with large pores, while acetone, tetrahydrofurane, ethyl propionate, ethyl acetate or dioxane led to monoliths with very small or no pores [6,30]. This effect was found to be related mainly to the difference in the solubility of the monomer and the porogen: the larger it is, the larger pores will form [10]. In contrast, similar solubilities will result in nanoporous or bulk structures.

In addition to single solvents, their combinations could also lead to the formation of monoliths with specific properties. This case is especially interesting when the mixture is formed by a poor (large difference in the solubilities of the solvent and the monomer) and a good solvent (close solubilities). While solubility could be a selection criterion for solvent(s) in some monolith systems, other parameters, like dipole moment, partition coefficient (log P) or polarity index (PI) have also been proposed [24]. However, none of them can be considered omnipotent: for some monoliths the dipole moment works best, while for others it is better to use the solubility parameter.

In this study the effect of the binary mixture of a macropore forming solvent (methanol) with nanopore or bulk forming solvents (acetone, acetonitrile and ethyl acetate) is investigated for diethylene glycol dimethacrylate polymer monoliths prepared by gamma radiation-initiated polymerization. The morphology of the formed structures was studied, together with the polymerization kinetics obtained from irradiation dose-dependent conversion curves. Our aim is to evaluate the formation of bulk and macroporous monoliths from the same monomer in different solvents through the interpretation of the reaction kinetics in the context of the Avrami approach, and to determine the effect of the composition of binary solvent mixtures on the growth and porous structure of the monoliths.

2. Materials and methods

Diethylene glycol dimethacrylate (DEGDMA, Sigma Aldrich) monomer was used for the preparation of the monoliths with methanol (MetOH, AnalityCals, Carlo Erba), acetone (AC, Reanal), acetonitrile (AN, Carlo Erba), ethyl acetate (EtAc, Reanal) porogens. All chemicals were HPLC grade and used as received. The solubility parameters of these materials are given in Table 1.

The monoliths were prepared by using in situ gamma-radiation initiated polymerization. Approx. 25 mm long and 4 mm ID Teflon tubes were placed in plastic bags that were filled with deoxygenated solution of the monomer in the solvents of different composition and sealed in nitrogen atmosphere. The samples were irradiated with a ^{60}Co γ-source at room temperature. The total absorbed dose was set between 1 and 22 kGy, with a dose rate of 11 kGy/h. The dose and dose rate values were determined by using ethanol–-chlorobenzene dosimeter solution. All monoliths were prepared in duplicates, and the same irradiation experiments were repeated several times. After the irradiation, the tubes were removed from the bags, and cleaned from the polymer that is formed outside the tube. Then, the tube was attached to a Liquochrom Model 2010 (LMIM, Hungary) chromatographic pump via standard chromatography fittings. Solvent was pumped through the tube to clean the monolith from the unreacted monomers and the solvent. During these experiments, the monoliths in the tubes were swollen due to the presence of the solvent. This prevented them from coming out of the Teflon tubes under pressure. When they were left drying out in the tubes, it was easy to remove the polymer from the tubes.

The morphology of the samples was studied using a JEOL JSM 5600LV (Tokyo, Japan) scanning electron microscope (SEM). Approximately 1 mm thick samples cut from the monolith were fixed to the sample holder, and sputter-coated with platinum/palladium by using a JEOL JFC-1300 Auto Fine Coater (Tokyo, Japan).

Table 1
Solubility parameters of the materials used in this study.

Material	Solubility parameter (MPa$^{1/2}$) [31]
Diethylene glycol dimethacrylate – DEGDMA	9.8
Acetone – AC	19.7
Acetonitrile – AN	12.5
Ethyl acetate – EtAc	18.2
Methanol – MetOH	29.7

Mercury porosimetry measurements, performed on a Carlo Erba Pascal 140 (Milan, Italy) was used to determine the average pore size, while nitrogen absorption measurements for the specific surface area were done on a Micromeritics, ASAP 2000 (Norcross, USA) instrument.

The conversion of the monomer was calculated by comparing the weight of the crosslinked polymer to the weight of the initial monomer in the feed solution. The weight measurements were performed on a micro-scale. The polymerization times were obtained from the dose and the dose rate values.

The conversion data were fitted with the Avrami equation [32]:

$$y(t) = a\,(1 - \exp(-kt^n)), \tag{1}$$

where a is a correction factor, k is the Avrami constant related to the reaction rate, and n is the Avrami exponent. For a polymerization process, the reaction rate k is dependent on the nucleation rate and the propagation rate. The Avrami exponent n is determined by the character of the nucleation and propagation. In general, its values are ranging from 1 to 4, being characteristic for different growth mechanisms [33], however, anomalous Avrami exponent values, even of >20 were also reported [34].

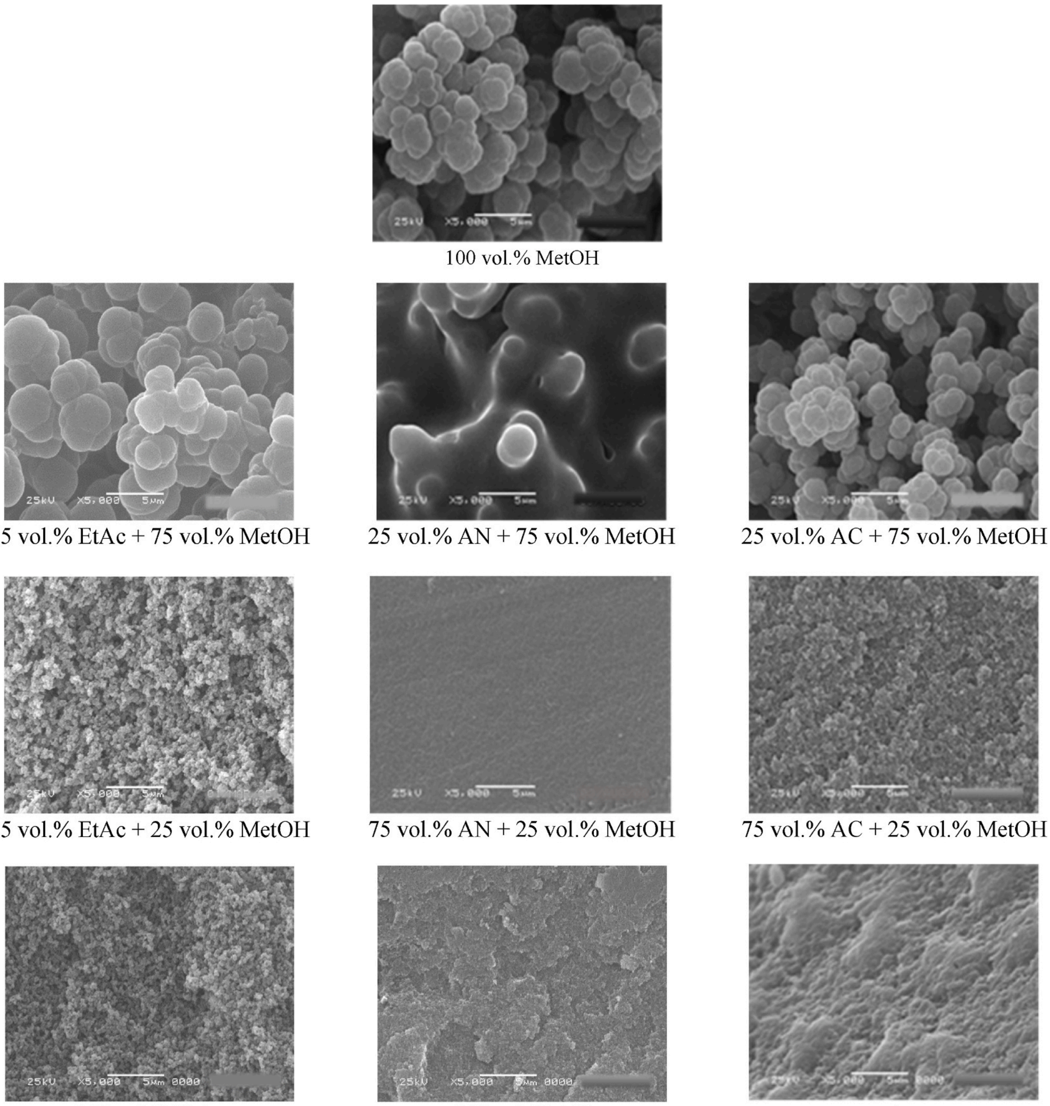

100 vol.% MetOH

25 vol.% EtAc + 75 vol.% MetOH

25 vol.% AN + 75 vol.% MetOH

25 vol.% AC + 75 vol.% MetOH

75 vol.% EtAc + 25 vol.% MetOH

75 vol.% AN + 25 vol.% MetOH

75 vol.% AC + 25 vol.% MetOH

100 vol.% EtAc

100 vol.% AN

100 vol.% AC

Fig. 1. Morphology of the samples prepared with 30 vol% DEGDMA and 70 vol% binary porogen system of MetOH with EtAc, AN, and AC, respectively. The captions show the composition of the solvent mixture. The irradiation was performed with 22 kGy dose and 11 kGy/h dose rate.

3. Results and discussion

The morphology of some typical samples from the EtAc/MetOH, AN/MetOH and AC/MetOH binary porogen mixtures can be seen on scanning electron microscopy images in Fig. 1. The use of pure alcohol, being a poor solvent for DEGDMA (and so a good porogen for the monolith), results in a macro- and microporous structure with channels of a few or a few tens of microns. The formed polymer consists of micron-sized microglobules agglomerated into larger clusters. This morphology is the result of the precipitation polymerization process: the microglobules are the nuclei that precipitated from the solution, that are coalescing and/or growing further by the attachment of the monomers to their surface.

The addition of the second porogen (a good solvent for DEGDMA, see Table 1) to the mixture in small (25 vol%) concentrations causes minimal changes in the porous properties for the EtAc/MetOH and AC/MetOH systems, but the morphology of aggregated microglobules almost completely disappears in the sample prepared with the AN/MetOH mixture. Here, some microparticles can be recognized but the surface is generally smooth, yet pores can be observed.

The further increase of the concentration to 50 vol% leads to nanoporous (EtAc, AC) and bulk (AN) structures, and this tendency continues towards the monomer mixtures containing only the second (good) solvent. At 100 vol% solvent concentrations recognizable pores and porous structure can be observed for the EtAc sample only.

The above-described changes in the morphology and porosity of the monoliths affect their flow-through characteristics, and therefore, are critical parameters in the most widespread applications of these polymers – chromatographic separation media. It can be concluded that the average pore size can be increased and even doubled by the addition of AC, AN or EtAc solvent to the alcohol in small concentrations (20–30 vol%). In this regard, they can be used to tune the (macro)porous properties of DEGDMA monoliths to specific chromatographic needs. Higher concentrations of these solvents, however, lead to a rapid decrease in average pore sizes. Above certain concentrations, the obtained bulk polymers with micro- and nanopores will have low permeability, not suitable for chromatographic applications.

The average pore size and specific surface are values of the samples are shown in Table 2. These measurements were performed on samples with 0, 20, 30 and 40 vol% solvent concentrations. As it can been seen on the SEM image, the single-solvent MetOH/DEGDMA monolith is mesoporous with average pore size of 3.54 μm and surface area of 1.7 m^2/g. Interestingly, the addition of the second solvents in small (20 vol%) concentrations results in structures with larger average pore sizes and smaller specific surfaces. For 30 vol% concentrations the average pore size slightly increases and decreases for EtAc and AC, respectively, while drops by cca. 35 times in the case of AN. Further increase of the concentration causes rapid drop of the pores to the nanopore range for AN and AC (26 and 111 nm, respectively), while it is 590 nm for the EtAc sample. At 100 vol% solvent concentrations pores were detected only in the EtAc sample. These findings are in good agreement with the contents of the SEM images.

Three different binary solvent systems were used in different concentrations for DEGDMA monolith preparation: ethyl acetate/methanol, acetonitrile/methanol and acetone/methanol. The dependence of the conversion on the irradiation time (which is proportional to the gamma-radiation dose, with the 11 kGy/h dose rate coefficient) for the three systems is shown in Fig. 2. It can be seen that the conversion is minimal at very low doses (0.1 and 0.2 h irradiation times), then increases rapidly, and reaches a plato after 0.4–1.0 h of treatment, depending on the type and composition of the porogen. A nearly 100 % conversion can be achieved for all three systems and all compositions after 1.5 h of gamma-irradiation (corresponding to 16 kGy dose).

The experimental data were fitted with the Avrami equation [24,32], describing the (liquid to solid) phase transformation of the materials at a constant temperature. This formula is widely used to characterize crystallization and glass formation processes that are, in many aspects, analogous to the precipitation polymerization occurring during the DEGDMA monolith synthesis. Therefore, the fitting of the experimental data with the Avrami equation could help in understanding the monolith formation process. This approach has been used for the gamma radiation-initiated polymerization of DEGMA monoliths in different single-solvent systems earlier [35]. The results of the fitting with the Avrami equation are also shown in Fig. 2.

As Fig. 2 illustrates, the change of the conversion with the irradiation time (or the rate of the polymerization) is affected by both the type and the composition of the binary solvent. Fig. 3 shows the dependence of the Avrami constant, related to the nucleation rate and growth rate [36], on the content of the second solvent in the monomer mixture. It can be seen that for 0 vol% of second solvent (corresponding to 100 vol% of methanol) the nucleation and growth rates, and so the monolith formation is relatively slow ($k = 1.71$/hr). Similarly small Avrami constant values were obtained for the monomer mixtures prepared purely with the second solvents. Here EtAc and AC have very similar values ($k = 1.57$ and 1.61/hr, respectively), while for AN it is slightly higher ($k = 1.81$/hr).

However, k has a bell-shaped behavior in-between, with the highest values being almost double of the above-mentioned ones, 3.13, 3.00 and 3.22 for 50 vol% EtAc, AC and AN, respectively. It can be seen that the use of solvent mixtures under the same conditions

Table 2
Average pore diameter and specific surface are values for the single- and double-solvent DEGDMA monoliths.

Solvent in MetOH, vol%	Avg. pore diameter, nm/$S_{BET,}$ m/g^2		
	AC	AN	EtAc
0		3540/1.7	
20	5276 / 1.2	7193 / 0.9	6451 / 0.97
30	4622 / 1.4	189 / 31.0	6834 / 0.94
40	111 / 43.0	26 / -	590 / 10.4
100	-/-	-/-	85 / 24.2

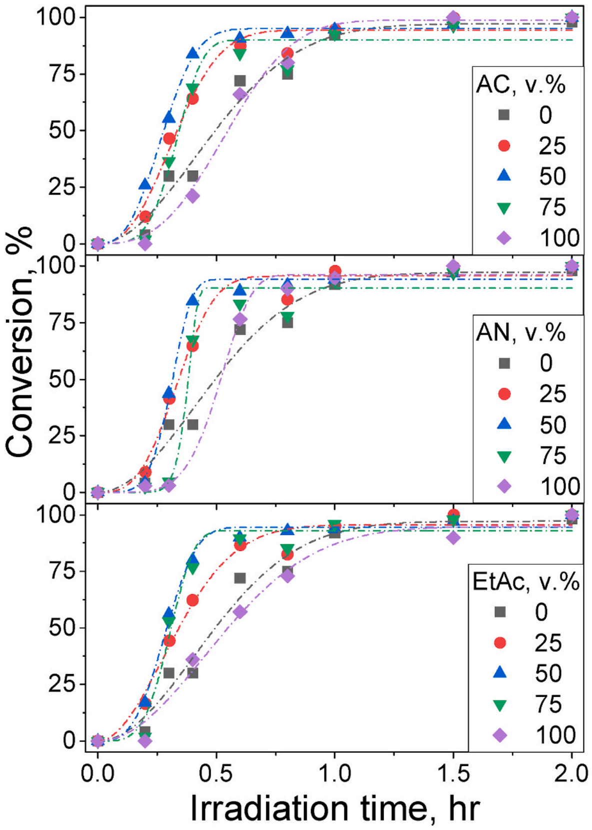

Fig. 2. Conversion of the DEGDMA monolith with the irradiation time for monomer mixtures consisting of the monomer and ethyl acetate/methanol (bottom), acetonitrile/methanol (center) and acetone/methanol (top) binary solvent mixtures of different composition. The symbols indicate the experimental results, while the dash-dot curves correspond to the fitted Avrami functions.

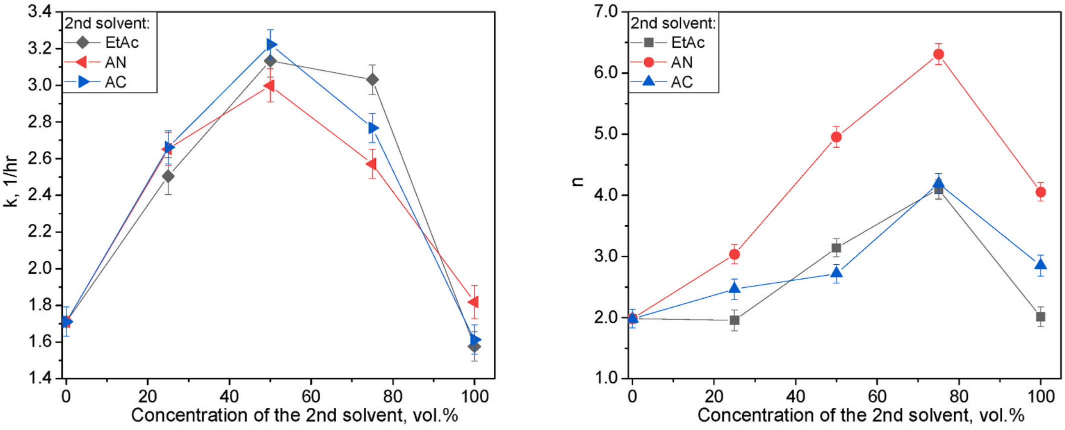

Fig. 3. Dependence of the (left) Avrami constant and the (right) Avrami exponent on the concentration of the second solvent in the binary porogen system of ethyl acetate, acetonitrile and acetone with methanol.

results in higher nucleation and growth rates, compared to the single-solvent cases for all three porogen systems. Presumably this is the reason for the larger pores observed by the pore size measurements in the samples with low concentrations of the second solvent, where the pore formation is still dominated by the poor solvent (MetOH).

The change of the Avrami exponent n with the composition of the solvent mixture is also shown in Fig. 3. The Avrami exponent reflects the nucleation and growth mechanisms during the polymerization [36,37]. In the case of pure methanol porogen the value of 2 for n is characteristic for nucleation on the surface, accompanied by one-dimensional growth [38,39]. As EtAc, AN and AC are added to the solvent mixture in increasing concentrations the Avrami exponent increases. For EtAc and AC it has similar values, reaching 2.7–3.1 for the 50 vol% case and the maximum value of 4.2 for the compositions with 75 vol% EtAc and AC content. This behavior indicates the transformation of the growth from one-dimensional first to two- ($n \sim 3$) and then to three-dimensional ($n \sim 4$), depending on the concentration of the second solvent in the mixture. Interestingly, with pure EtAc the growth switches back to one- ($n \sim 2.0$), while with pure AC to two-dimensional ($n \sim 2.9$) mechanism.

Compared to EtAc and AC, the Avrami exponent increases faster with acetonitrile concentration. n is 3.0, 5.0 and 6.3 for 25, 50 and 75 vol% of AN, respectively, and decreases to 4.1 in the pure single-solvent case. In general, values of the Avrami exponent exceeding 4.0 are treated as anomalous [39,40], and interpreted as indication of fractal growth mechanism with non-constant nucleation and growth rates. In 100 vol% AN the growth mechanism becomes three-dimensional.

The fitting results of the conversion curves give some insights on the growth mechanism of monoliths with binary porogen mixtures. In pure MetOH, being a poor solvent for DEGDMA resulting in microporous monolith formation, the growth mechanism is one-dimensional, as it would be expected for the precipitation polymerization. The other solvents are bulk or nano-porous polymer-forming solvents for DEGDMA, and the growth mechanism for 100 vol% concentrations of EtAc, AC and AN is one-, two- and three-dimensional, respectively. The use of solvent mixtures increases the dimensionality of growth and the growth rate in all cases. This behavior is especially remarkable for AN, where it leads to fractal growth with a growth rate being smaller than for EtAc and AC.

4. Conclusions

Binary porogen mixtures of ethyl acetate/acetone/acetonitrile with methanol were used to synthesize diethylene glycol dimethacrylate polymer monoliths with gamma radiation-initiated polymerization. The effect of the composition of the solvent mixture on the morphology, pore size and specific surface area, and the reaction kinetics, including the growth mechanism and the growth rate was studied with the irradiation dose-dependent conversion profiles. It was found that the use of solvent mixtures almost doubles the polymerization rate, compared to the single solvents. Binary solvent ratios dominated by methanol cause the formation of larger pores in the monoliths. The addition of the second solvent also changes the growth mechanism by increasing its dimensionality in all cases, from one- (solely methanol and solely ethyl acetate solvents) and two-dimensional (solely acetone) to three-dimensional (solely acetonitrile, and binary porogens of 25 vol% methanol + 75 vol% ethyl acetate and 25 vol% methanol + 75 vol% acetone). A fractal growth mechanism has been identified for the 25 vol% methanol + 75 vol% acetonitrile binary solvent mixture.

Our results show that the use of binary solvent mixtures of a poor and a good solvent has several advantages in the preparation of dimethacrylate porous monoliths with gamma radiation-induced polymerization. Changing the ratio of the two solvents allows to control the growth mechanism of the polymer growth in a broad range. It can be used to tune the pore size, and even to increase it compared to the single-solvent case. The reaction kinetics can be interpreted by the Avrami equation in a broad range of solvents and solvent mixture compositions. The obtained Avrami parameters are in good agreement with the findings of the morphology and pore size measurements of the formed monoliths.

Funding

The work was partially supported by the Ministry of Culture and Innovation of Hungary from the National Research, Development and Innovation Fund (NKFIH) via INBIOM TKP2021-EGA-04 and TKP2021-NVA-04 grants, and by the ELKH-KKT-2021 grant of the Eötvös Loránd Research Network.

Data availability statement

Data will be made available on request.

CRediT authorship contribution statement

Barbara Beiler: Writing – review & editing, Methodology, Investigation, Data curation, Conceptualization. **Ágnes Sáfrány:** Methodology. **Lilia Bató:** Investigation. **Zsombor Szomor:** Investigation. **Miklós Veres:** Writing – original draft, Visualization, Conceptualization.

Declaration of competing interest

The authors declare that they have no known competing financial interests or personal relationships that could have appeared to influence the work reported in this paper.

Acknowledgements

The authors of this paper wish to thank Z. Papp for the irradiation of the samples.

References

[1] S. Poddar, S. Sharmeen, D.S. Hage, Affinity monolith chromatography: a review of general principles and recent developments, Electrophoresis 24 (2021) 2577–2598. https://doi:10.1002/elps.202100163.

[2] E. Lubomirsky, A. Khodabandeh, J. Preis, M. Susewind, T. Hofe, E.F. Hilder, R.D. Arrua, Polymeric stationary phases for size exclusion chromatography: a review, Anal. Chim. Acta 1151 (2021) 338244, https://doi.org/10.1016/j.aca.2021.338244.

[3] X. Ding, J. Yang, Y. Dong, Advancements in the preparation of high-performance liquid chromatographic organic polymer monoliths for the separation of small-molecule drugs, J. of Pharm. Anal. 8 (2018) 75–85. https://doi:10.1016/j.jpha.2018.02.001.

[4] J.C. Masini, Separation of proteins by cation-exchange sequential injection chromatography using a polymeric monolithic column, Anal. Bioanal. Chem. 408 (2016) 1445–1452. https://doi:10.1007/s00216-015-9242-9.

[5] M. Szumski, B. Buszewski, Preparation of monolithic capillary chromatographic columns using supercritical fluid as a porogen solvent, Chromatog 77 (2014) 1009–1017, https://doi.org/10.1007/s10337-014-2651-7.

[6] E.C. Peters, F. Svec, J.M.J. Fréchet, Rigid macroporous polymer monoliths, Adv. Mat. 11 (1999) 1169–1181, https://doi.org/10.1002/(SICI)1521-4095(199910)11:14<1169::AID-ADMA1169>3.0.CO;2-6.

[7] M. Grasselli, E. Smolko, P. Hargittai, Á. Sáfrány, From microsheres to monoliths: synthesis of porous support with tailored properties, Nucl. Instrum. Methods B 185 (2001) 254–261, https://doi.org/10.1016/S0168-583X(01)00839-4.

[8] Á. Sáfrány, B. Beiler, K. László, F. Svec, Control of pore formation in macroporous polymers synthesized by single-step γ-radiation-initiated polymerization and cross-linking, Polymer 46 (2005) 2862–2871, https://doi.org/10.1016/j.polymer.2005.02.024.

[9] B. Beiler, Á. Vincze, F. Svec, Á. Sáfrány, Poly(2-hydroxyethyl acrylate-co-ethyleneglycol dimethacrylate) monoliths synthesized by radiation polymerization in a mold, Polymer 48 (2007) 3033–3040. https://doi:10.1016/j.polymer.2007.04.002.

[10] Á. Sáfrány, B. Beiler, Radiation Synthesized Functional Polymer Supports with Taiormade Properties for Separation and Purification, IAEA TECDOC-1465, 2005, pp. 53–67.

[11] Y.-P. Zhang, L.-Q. Fan, K.-P. Lee, Y.-J. Zhang, S.-H. Choi, W.-J. Gong, Preparation of monolithic capillary columns for capillary electrochromatography by γ-ray irradiation, Microchim. Acta 158 (2007) 353–360. http://doi:10.1007/s00604-006-0694-7.

[12] P. Simone, G. Pierri, P. Foglia, F. Gasparrini, G. Mazzoccanti, A.L. Capriotti, A. Laganà, Separation of intact proteins on γ-ray-induced polymethacrylate monolithic columns: a highly permeable stationary phase with high peak capacity for capillary high-performance liquid chromatography with high-resolution mass spectrometry, J. of Sep. Sci. 39 (2015) 264–271, https://doi.org/10.1002/jssc.201500844.

[13] P. Simone, G. Pierri, D. Capitani, A. Ciogli, G. Angelini, O. Ursini, F. Gasparrini, Capillary methacrylate-based monoliths by grafting from/to γ-ray polymerization on a tentacle-type reactive surface for the liquid chromatographic separations of small molecules and intact proteins, J. of Chrom. A. 1498 (2017) 46–55, https://doi.org/10.1016/j.chroma.2016.11.039.

[14] M. Volokitina, M. Krutyakova, V. Sirotov, M. Larionov, T. Tennikova, E. Korzhikova-Vlakh, Protein biochips based on macroporous polymer supports: material properties and analytical potential, J. Pharm. Biomed. Anal. 165 (2019) 242–250, https://doi.org/10.1016/j.jpba.2018.12.012.

[15] R. Bakry, G.K. Bonn, D. Mair, F. Svec, Monolithic porous polymer layer for the separation of peptides and proteins using thin-layer chromatography coupled with MALDI-TOF-MS, Anal. Chem. 79 (2007) 486–493, https://doi.org/10.1021/ac061527i.

[16] F. Svec, Porous polymer monoliths: amazingly wide variety of techniques enabling their preparation, J. Chromatogr. A. 1217 (2010) 902–924, https://doi.org/10.1016/j.chroma.2009.09.073.

[17] E. Badaloni, M. Barbarino, W. Cabri, I. D'Acquarica, M. Forte, F. Gasparrini, F. Giorgi, M. Pierini, P. Simone, O. Ursini, C. Villani, Efficient organic monoliths prepared by γ-radiation induced polymerization in the evaluation of histone deacetylase inhibitors by capillary(nano)-high performance liquid chromatography and ion trap mass spectrometry, J. Chrom. A 1218 (2011) 3862–3875, https://doi.org/10.1016/j.chroma.2011.04.048.

[18] P. Simone, G. Pierri, P. Foglia, F. Gasparrini, G. Mazzoccanti, A.L. Capriotti, O. Ursini, A. Ciogli, A. Laganà, Separation of intact proteins on γ-ray-induced polymethacrylate monolithic columns: a highly permeable stationary phase with high peak capacity for capillary high-performance liquid chromatography with high-resolution mass spectrometry, J. Sep. Sci. 39 (2016) 264–271, https://doi.org/10.1002/jssc.201500844.

[19] M.H. Mohamed, L.D. Wilson, Porous copolymer resins: tuning pore structure and surface area with non reactive porogens, Nanomat 2 (2012) 163–186, https://doi.org/10.3390/nano2020163.

[20] Y. Li, H.D. Tolley, M.L. Lee, Poly[hydroxyethyl acrylate-co-poly(ethylene glycol) diacrylate] monolithic column for efficient hydrophobic interaction chromatography of proteins, Anal. Chem. 81 (2009) 9416–9424, https://doi.org/10.1021/ac9020038.

[21] X. Wang, X. Lin, Z. Xie, Preparation and evaluation of a sulfoalkylbetaine-based zwitterionic monolithic column for CEC of polar analytes, Electrophor 30 (2009) 2702–2710, https://doi.org/10.1002/elps.200900006.

[22] S. Yu, F. Ng, K. Ma, A. Mon, F. Ng, Y. Ng, Effect of porogenic solvent on the porous properties of polymer monoliths, J. Appl. Polym. Sci. 127 (2012) 2641–2647, https://doi.org/10.1002/app.37514.

[23] M.R. Buchmeiser, Polymeric monolithic materials: syntheses, properties, functionalization and applications, Polym 48 (2007) 2187–2198, https://doi.org/10.1016/j.polymer.2007.02.045.

[24] F.R. Mansour, S. Waheed, B. Paull, F. Maya, Porogens and porogen selection in the preparation of porous polymer monoliths, J. Sep. Sci. 43 (2020) 56–69, https://doi.org/10.1002/jssc.201900876.

[25] F. Svec, J.M.J. Fréchet, Temperature, a simple and efficient tool for the control of pore size distribution in macroporous polymers, Macromol 28 (1995) 7580–7582, https://doi.org/10.1021/ma00126a044.

[26] C. Viklund, F. Svec, J.M.J. Fréchet, K. Irgum, Monolithic, "molded", Porous Materials with High Flow Characteristics for Separations, Catalysis, or Solid-Phase Chemistry: Control of Porous Properties during Polymerization, Chem. Mater. 8 (1996) 744–750, https://doi.org/10.1021/cm950437j.

[27] Y. Naka, Y. Yamamoto, Preparation of copolymer microspheres of diethylene glycol dimethacrylate, J. of Polym. Sci. Part A: Polymer Chemistry 30 (1992) 2149–2158, https://doi.org/10.1002/pola.1992.080301008.

[28] Y. Naka, I. Kaetsu, Y. Yamamoto, K. Hayashi, Preparation of microspheres by radiation-induced polymerization. I. Mechanism for the formation of monodisperse poly(diethylene glycol dimethacrylate) microspheres, J. of Polym. Sci. Part A: Polymer Chemistry 29 (1991) 1197–1202, https://doi.org/10.1002/pola.1991.080290814.

[29] Y. Suzhu, L.N. Fern, C.C.M. Khin, A.M. Aye, L.N. Feng, Y.N. Yen, Effect of porogenic solvent on the porous properties of polymer monoliths, J. Appl. Polym. Sci. 127 (2013) 2641–2647, https://doi.org/10.1002/app.37514.

[30] Y. Li, H.D. Tolley, M.L. Lee, Preparation of monoliths from single crosslinking monomers for reversed-phase capillary chromatography of small molecules, J. Chrom.A 1218 (2011) 1399–1408, https://doi.org/10.1016/j.chroma.2011.01.028.

[31] Handbook of Solubility Parameters, CRC Press, 1983.

[32] J. Málek, T. Mitsuhashi, Testing method for the Johnson-Mehl-Avrami equation in kinetic analysis of crystallization processes, J. Am. Ceram. Soc. 83 (2000) 2103–2105, https://doi.org/10.1111/j.1151-2916.2000.tb01523.x.

[33] N.P. Bansal, C.H. Drummond III, Kinetics of hexacelsian-to-celsian phase transformation in SrAl2Si2O8, J. Am. Ceram. Soc. 76 (1993) 1321–1324, https://doi.org/10.1111/j.1151-2916.1993.tb03758.x.

[34] S. Sohrabi, R. Gholamipour, Effect of Nb minor addition on the crystallization kinetics of Zr-Cu-Al-Ni metallic glass, J. Non-Cryst. Solids 560 (2021) 120731, https://doi.org/10.1016/j.jnoncrysol.2021.120731.

[35] M.H. Mahmood, L. Himics, T. Váczi, I. Rigó, R. Holomb, B. Beiler, M. Veres, Raman spectroscopic study of gamma radiation-initiated polymerization of diethylene glycol dimethacrylate in different solvents, J. of Raman Spect. 52 (2021) 1735–1743, https://doi.org/10.1002/JRS.6207.

[36] K.G.F. Janssens, D. Raabe, E. Kozeschnik, M.A. Miodownik, B. Nestler, Computational Materials Engineering – an Introduction to Microstructure Evolution, Elsevier B.V., London, 2007.

[37] A. Pratap, K.G. Raval, A. Gupta, S.K. Kulkarni, Nucleation and growth of a multicomponent metallic glass, Bull. Mater. Sci. 23 (2000) 185–188, https://doi.org/10.1007/BF02719907.

[38] K. Shirzad, C. Viney, A critical review on applications of the Avrami equation beyond materials science, J. R. Soc. Interface. 20 (2023) 20230242, https://doi.org/10.1098/rsif.2023.0242.

[39] P. Zemenová, R. Král, M. Rodová, K. Nitsch, M. Nikl, Calculations of Avrami exponent and applicability of Johnson–Mehl–Avrami model on crystallization in Er: LiY(PO3)4 phosphate glass, J. Therm. Anal. Calorim. 141 (2020) 1091–1099, https://doi.org/10.1007/s10973-019-09068-w.

[40] M. Malekan, R. Rashidi, S.G. Shabestari, Mechanical properties and crystallization kinetics of Er-containing Cu–Zr–Al bulk metallic glasses with excellent glass forming ability, Vacu 174 (2020) 109223, https://doi.org/10.1016/j.vacuum.2020.109223.